Journal of the European Ceramic Society 45 (2025) 117001

Contents lists available at ScienceDirect

Journal of the European Ceramic Society

journal homepage: www.elsevier.com/locate/jeurceramsoc

The role of alignment for valid tensile testing of ceramic matrix composites

Stefan Flauder *, Nico Langhof, Stefan Schafföner

Chair of Ceramic Materials Engineering (CME), University of Bayreuth, Prof.-Rüdiger-Bormann-Str. 1, Bayreuth 95447, Germany

ARTICLE INFO

Keywords:
Alignment
Ceramic matrix composites (CMCs)
Mechanical properties
C/C-SiC
Tensile testing

ABSTRACT

The determination of tensile properties of ceramic matrix composites (CMCs) is crucial for material development and assessment. Despite the damage tolerance of CMCs, the efforts required for proper tensile testing are similar high than for ceramics. This study describes a method to determine the sample alignment prior every single tensile testing and discusses the required amount of alignment for valid testing. For this purpose, carbon fiber-reinforced silicon carbon (C/C-SiC) samples were evaluated by only two alignment criteria. Approximately 80 % of the tensile samples failed valid with a percentage bending less than 6 % and no valid testing was achieved at a percentage bending higher than 12.3 %. Invalid testing showed an increase of strength scattering of more than 50 %, but only a minor change of the strength. The preliminary alignment check and subsequent realignment was able to increase the rate of validly tested samples by about four times.

1. Introduction

The need for materials to withstand harsh environments and high temperatures has led to the development of continuous fiber-reinforced ceramic matrix composites (CMCs). These materials are characterized by high resistance to temperature, thermal shock, wear, oxidation, as well as mechanical stress [1,2]. Consequently, CMCs play a key role for high loaded applications in aerospace [3] and tribology [4]. They are used in existing civilian aircraft engines [5] as a strategy to achieve higher efficiency, which has already been confirmed by a reduction of fuel consumption and greenhouse gas emission [6,7]. Since CMC are used in highly demanding conditions, the further expansion of CMC applications requires appropriate mechanical characterization and evaluation.

Similar to monolithic ceramics, the analysis of mechanical properties of CMCs is usually carried out using bending tests [8,9]. Bending tests require only a limited amount of effort in both sample preparation and testing. Therefore, bending tests have often been used for the development of new CMC materials, the evaluation of material performance, and their processes [10–17]. In contrast to bending tests with concurrent tensile and compressive stresses, tensile testing leads to a uniform stress distribution. Tensile tests are therefore essential, especially for studying static and cyclic fatigue phenomena of CMCs including the performance of additional environmental barrier coatings [18,19] and at high temperatures [20,21]. Even so, tensile testing requires accurate gipping of the samples and thus a proper alignment of the samples to exclude parasitic bending and other deviation from a pristine tensile load.

The detrimental effect of misalignments like bending on the tensile testing was studied and quantified in detail for monolithic ceramics [22,23]. This led to clear recommendations and methods for the determination of misalignments [22,24], as well as technical solutions for gripping devices and sample alignments to avoid the main sources of misalignments [25]. Finally, it was recommended for monolithic ceramics that a percentage bending of no more than 5 % during tensile testing can be accepted to achieve valid testing and the sample dimensional tolerances need to be less than 5 μm [22]. In contrast to monolithic ceramics, CMCs have an improved damage tolerant failure behavior with much higher strain to failure [1,2]. Additionally, only moderate sensitivity to misalignment has been suggested for CMCs [26]. Since no studies of the effect of bending, i.e. misalignment, on tensile strength testing exist for CMCs [27], the conservative percentage bending value for monolithic ceramics of 5 % was also set for tensile testing of CMCs [26,27].

Minor deviations from perfect specimen shapes are sometimes inevitable or have to be accepted for tensile testing of CMCs. These deviations in geometry are caused by the need to test samples with additional seal coatings [28], after sandblasting and application of environmental barrier coatings [18,19], or with the surface conditions in the as received state [29].

The regulations to determine the degree of misalignment for tensile specimens with rectangular cross section usually require the use of four [22] to twelve [24] strain gauges glued on the sample surfaces. This procedure can be very time-consuming for a large number of tested

* Corresponding author.
E-mail address: Stefan.Flauder@uni-bayreuth.de (S. Flauder).

https://doi.org/10.1016/j.jeurceramsoc.2024.117001
Received 11 September 2024; Received in revised form 15 October 2024; Accepted 18 October 2024
Available online 20 October 2024

samples. However, optical strain measurements as an alternative to strain gauges and clip-on extensometers can be used without manipulation or marking of the sample surface [30,31].

The aim of this study is therefore to evaluate and measure the influence of misalignments during tensile testing of CMCs on the validity of testing and their mechanical properties. Furthermore, the requirements and methods needed for valid tensile testing of samples with deviations from a perfect sample geometry are investigated. Consequently, one objective of this study was the development of a method to estimate and correlate misalignments resulting in invalid tensile failure outside the gauge length. For this approach carbon fiber-reinforced silicon carbon (C/C-SiC) tensile samples were preloaded and two verification criteria determined by optical strain measurement were developed and used to classify the alignment. The verification criteria were able to identify detrimental misalignment and allowed the samples to be realigned prior to final tensile testing.

2. Material and methods

Tensile samples were tested with concurrent alignment determination. The degree of measured misalignments was compared with the validity of tensile testing and the corresponding strength data to analyze their mutual dependencies and derive recommendations for appropriate tensile testing of CMCs. It is not the intention of this study to precisely determine, assign, and quantify misalignments like concentricity, angularity, or sample geometry deviations leading to S- or C-shape errors [25,26,32].

2.1. Material and tensile sample preparation

The ceramic matrix composite model material used in this study was a carbon fiber-reinforced silicon carbon (C/C-SiC). The C/C-SiC with continuous fiber reinforcement (HTA 40, Teijin Carbon Europe GmbH, Germany) was fabricated with plain-weave fabrics leading to a laminate with a fiber orientation in 0° and 90° (Fig. 1a). The material was made in-house at the Chair of Ceramic Materials Engineering in Bayreuth using the liquid silicon infiltration process (LSI) [33–35] and a thermoplastic matrix precursor [36–38]. Details of the used single manufacturing steps and processes for the material can be found elsewhere [29]. The microstructure of grounded and polished cross sections and the as received surfaces of C-C/SiC were analyzed by light microscopy (DSX1000, Olympus Corporation, Japan). The nominal fiber volume fraction of the C/C-SiC material was 51.3 ± 0.6 %. The C/C-SiC material had a skeletal density of 1.97 ± 0.01 g/cm^3 with an open porosity of 4.6 ± 0.9 %, determined by Archimedes' principle according to DIN EN 1389. Laminates were made with ten or twenty layers of fabric corresponding to C/C-SiC mean thicknesses of 2.52 ± 0.03 mm or 4.95 ± 0.02 mm, respectively. A total of eight square plates with a length of either 100 mm or 150 mm were fabricated. The standard deviation of the mean thicknesses with about 30 µm showed the high reproducibility of the production process. Nevertheless, it needs to be mentioned that maximum thickness differences within a single plate can be up to 100 µm. In principle, a grinding to parallel sample surfaces would be possible to diminish thickness variations. However, C/C-SiC laminates are anisotropic materials and especially grinding can damage the fibers in the load carrying direction on the surface. This can cause deviations of the measured from the intrinsic mechanical properties. Hence, one objective of this study was to determine the influence of the as received state on tensile testing, alignment, and the mechanical properties.

Two dog-bone like shapes were used for tensile and alignment testing (Fig. 1b and c). The longitudinal axes of the samples were always fabricated parallel to the 0° orientation of the reinforcing fibers with the tensile load applied in this direction (Fig. 1, red arrows). Tensile samples with these two geometries were prepared from plates with thicknesses of 2.52 and 4.95 mm, respectively, resulting in a total of four different sample sizes. The smaller shaped samples had a total length of 60.5 mm and a gauge width of 3.6 mm (Fig. 1b). The larger samples had a length of 77.4 mm and a gauge width of 5.4 mm (Fig. 1c). For final testing 55 samples were prepared with the smaller shape and 37 with the bigger shape. Both sample geometries were fabricated with the same gauge length of 20.0 mm, a transition radius of 90 mm, and an angle in the shoulder chamfer section of 8°. The geometry and especially the 8° chamfer were oriented on the recommendations of ASTM C1275 [27]. The precise angle of the shoulder was necessary as it was congruent with the chamfer in the gripping system resulting in an edge-loading and alignment of the samples by the shoulders. The high manufacturing precision of the 2-D sample contour as well as negligible machining forces [39] were achieved by electrical discharge machining of the plate material. The surface of the plates and thus the surface of the tensile samples was not machined and remained in the as received condition. An additional aluminum (AlCuMg1, 3.1325) dummy sample of the smaller sample shape (Fig. 1**b**) and a thickness of 4.10 mm was prepared from rolled sheet material for reference measurements with an isotropic

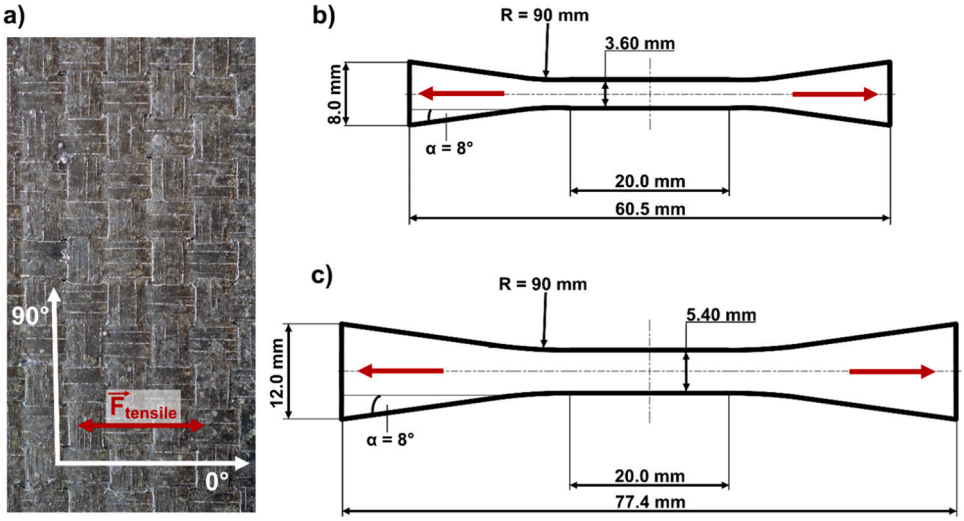

Fig. 1. a) As received C/C-SiC surface with clearly visible orientation of the 0° and 90° fiber bundles of the plain-weave fabric. The load was always applied parallel to the 0° direction. 2-D sample geometries for samples with a gauge width of b) 3.6 mm or c) 5.4 mm. Both sample shapes were tested with a thickness of 2.52 and 4.95 mm.

material of smooth surface.

2.2. Tensile testing and alignment

A universal test device (Z050 TEW 50 kN Allround floor, ZwickRoell Testing Systems GmbH, Austria) with a 10 kN load cell (Xforce K, ZwickRoell Testing Systems GmbH, Austria) was used for tensile and alignment testing. The load train was equipped with a test device designed for edge-loading and self-alignment of tensile samples described and evaluated in detail in a previous paper [29]. The main functions of this device are summarized in Fig. 2. Swivel heads were used to connect the tensile gripping units with the load train allowing some degree of free rotation (Fig. 2a). Consequently, torque that could arise by slightly twisted sample geometries can be minimized. The tensile samples were centered in the gripping by movable inserts with a system of congruent wedges independent from sample thickness (Fig. 2b). Finally, the edge-loaded samples were pulled, self-aligned and fixed in the gripping by using identical wedge angles of the sample and the gripping (Fig. 2c). Due to the intended use of samples with as received surfaces, the centering of the sample in the gripping by movable inserts had some adjustability in absolute positioning. This absolute positioning was changed by detaching and re-mounting of the samples. Hence, the re-mounting of samples in the alignment device were repeated until an optimum alignment was achieved for the single sample.

The alignment was measured with the method described in Section 2.3. For this purpose, the tensile samples were repeatedly preloaded to 30 MPa. This was below the limit of 45–55 MPa reported for the deviation from the initial proportional stress strain curve for a similar fabric reinforced C/C-SiC material [29]. Additionally, a sample was also stepwise preloaded to 30 MPa, 100 MPa, and ultimate tensile load to evaluate the stress strain behavior and the load level required for alignment verifications according to ASTM C1275 [27]. The alignment verification needs to be done with a loading to a strain of 0.05 % or to one half of the strain at the onset of cumulative fracture process whichever is greater. Moreover, the aluminum dummy sample was preloaded several times far below its yield strength ($R_{p0.2}$ about 245 MPa) in the linear elastic region to 780 N or about 53 MPa. The monotonic tensile tests to failure after the alignment measurement as well as the preloading tests for alignment were carried out with a loading rate of 0.5 mm/min to the preload of 5 N and a subsequent loading to failure or preload level with 1 mm/min. The fracture locations were measured after detachment of the ruptured tensile samples with a caliper on the two fragments.

2.3. Alignment measurement

The alignment of preloaded tensile samples was examined with an optical strain measurement system (laserXtens 2–120 HT/TZ, ZwickRoell Testing Systems GmbH, Austria) [40]. The measurement system illuminated the sample surface with a green laser diode of 532 nm wavelength. A camera followed the movement of characteristic surface speckle patterns on different preset sample positions to calculate the longitudinal strain [30,31]. No additional markings were needed on the sample surface for the speckle-correlation technique. The telecentric optic of the laserXtens compensates a lateral movement of the sample in the field of view direction of the camera in the range of ± 1.5 mm in comparison to the focus plane. In contrast to established alignment standards and recommendations, which require four to sixteen strain gauges glued equispaced around all circumferential sides of the sample [22,24,26], the optical strain was measured from only one side (Fig. 3). The field of view of the camera covered the surface obtained after electrical discharge machining perpendicular to the rough as received surfaces. Hence, this surface was smooth and due to the manufacturing also precisely parallel to its opposite sample surface within the gauge section. Furthermore, it was expected that the highest misalignment from the samples came from the absolute position accuracy of the as received surfaces in the wedge alignment. The used field of view

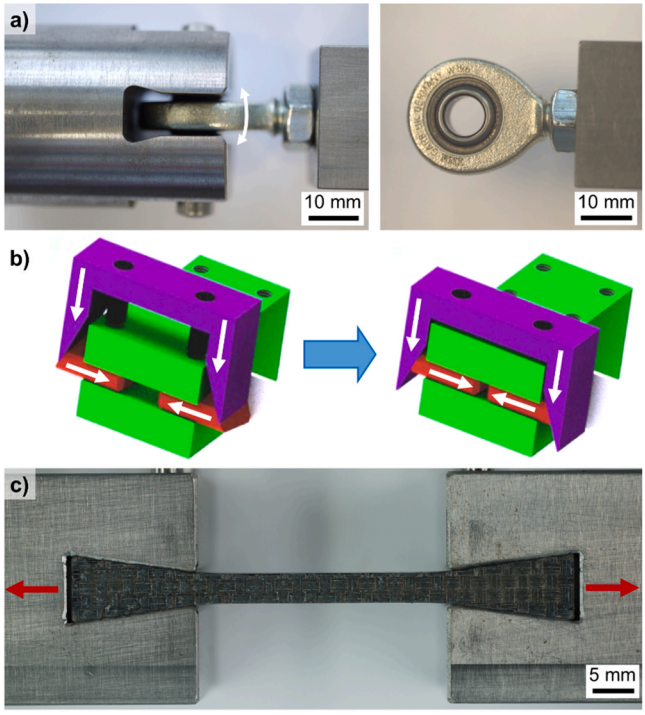

Fig. 2. a) Swivel head connect gripping with free rotation (± 5°) relative to the load train; b) Guided wedges (purple) and movable brass inserts (red) with congruent chamfers for centering of tensile samples in the gripping; c) Principle of self-alignment and fixation of the tensile specimen (black) in the gripping (metallic gray) using identical wedge angles.

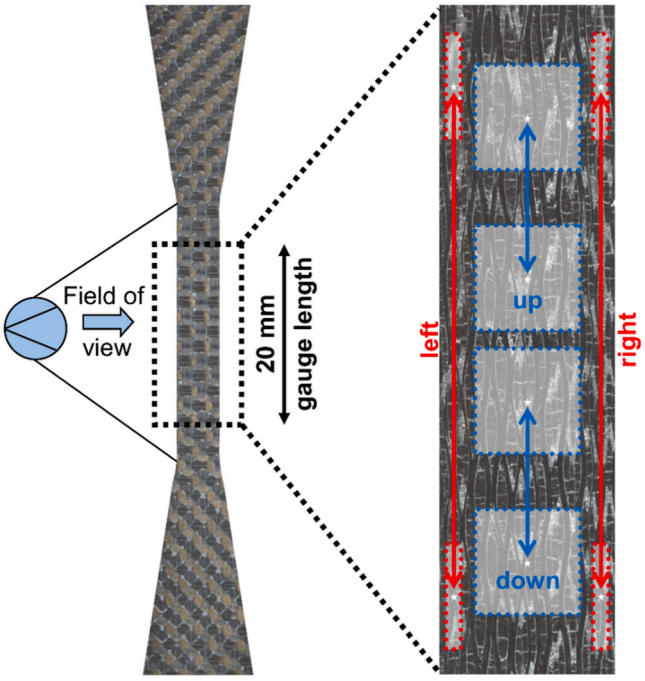

Fig. 3. Optical measurement of the strain within the gauge section: The percentage of bending was calculated from the strains measured on the outer left and right positions at a measurement length of 16.5 mm (red). The strain difference of up and down positions (blue) were determined at a measurement length of 5 mm.

perpendicular to the as received surfaces had therefore the highest sensibility to measure these misalignments.

For the quantification of the misalignment two different criteria were used: First, the percentage of bending (PB) between the left and the right side (Eq. 2.1) and secondly the strain difference between an up and down measurement position (Eq. 2.2) in the gauge section. For both criteria the samples were preloaded in the elastic region. To ensure the fixed state of sample mounting in the test device during repeated preloading, the load was only removed to a small residual of 0.5 N. The longitudinal strains were measured for the left (S_{left}) and right (S_{right}) side of the sample gauge section at a distance of 16.5 mm (Fig. 3, red). The up (S_{up}) and down (S_{down}) strains were determined at a measurement length of 5 mm (Fig. 3, blue). For S_{up}, the lowest measurement position was set 5 mm above the centerline of the 20 mm gauge section, whereas the highest measurement position of S_{down} was set 5 mm below the centerline of the gauge section. The strains of the four different measurement positions were determined at least for three loading repetitions to calculate the respective means ($\overline{S}$, Strain data are given in Supplementary material S1). For the PB value, the axial strain (S_{axial}) was quantified as the mean value of all strain measurements from the left and the right side.

$$PB = \left|\frac{(\overline{S_{left}} - \overline{S_{right}}}{S_{axial}} \bullet 100\right| \quad (2.1)$$

$$\Delta(up/down) = |(\overline{S_{up}} - \overline{S_{down}}| \quad (2.2)$$

The laserXtens achieved the highest resolution of 0.15 µm for a measurement point with a setting of an area of interest for the speckle observation larger than 128 pixels [31] in the strain direction. For this reason, the areas of interest were set to 256*256 pixels for the up and down and 40*256 pixels for the left and right measurements with the software (laserXtens, version 3.12.0.7, ZwickRoell Testing Systems GmbH, Austria). All strain measurements were performed with a data acquisition rate of the camera set to 70 Hz and a smoothing of raw data acquisition during the test by a moving average and a time parameter of 100 ms. Since no directional dependencies were observed for the strain analysis between left and right or up and down measurements, the alignment parameters of Eq. (2.1) and Eq. (2.2) were computed as absolute values.

According to standards and recommendations for tensile testing of monolithic ceramics and ceramic matrix composites, samples were found to be in the aligned state when the calculated percentage bending (PB) was less than 5 % [22,27]. Hence, this 5 % criterion was chosen as maximum allowable value for the left and right strain measurement. For the up and down strain criterion, the present gauge length of 20 mm restricted the measurement length to only 5 mm. This led to absolute strains of about 2.7 µm. For these small strains, the 5 % criterion was not sufficient as it was exceeded solely by the measurement uncertainty of about 0.15 µm. Consequently, the simple 5 % criterion was replaced by a maximum allowable strain difference of 0.45 µm, which was three times the measurement uncertainty and can be reliably distinguished by the measurement as misalignment. Preloaded tensile samples were detached and re-mounted in the testing device until fulfilment of the two alignment criteria was achieved. Subsequently, these samples with compliance of alignment were loaded until final failure. Some samples were not able to achieve compliance of alignment. Nevertheless, they were also tested to failure after being mounted in the best possible alignment condition measured.

3. Results and discussion

To investigate the role of alignment for valid tensile testing of CMCs, the method to check the alignment will be discussed first for the aluminum dummy sample and the C/C-SiC model material. The influence of the validity of tensile testing and its consequences for the obtained strength data of C/C-SiC is then evaluated. Finally, the interdependence of quantified sample alignment and the corresponding valid or invalid failure of CMC tensile samples will be discussed in detail.

3.1. Preloading of C/C-SiC samples and alignment measurement with aluminum dummy

As can be seen in Fig. 4, a characteristic stress-strain curve was observed for the monotonic tensile loading of the tested C/C-SiC samples. The deviation of the linear slope increased gradually above 50 MPa stress and 0.1 % strain until the sample fractured at 164 MPa. This deviation was attributed to the cracking of the matrix, a debonding of the fibers from the matrix, fiber cracking and fiber pull-out with increasing load, which is typical for ceramic matrix composites [2]. Below this blurred threshold, a linear-elastic behavior of the samples can be assumed. Hence, the preloading level for the alignment was set to 30 MPa.

To further ensure that damages in the samples due to the preloading during alignment verification can be neglected, a sample was stressed with increasing stages of load. Subsequently, the permanent strain was determined (Fig. 5). Compared to the permanent strain of 0.02 % measured after a high loading to 100 MPa, the permanent strain after a previous load to 30 MPa was negligible. Furthermore, the total strain at 30 MPa was only 0.06 %. Hence, the requirement for alignment determination according to ASTM C1275 [27], which requires the application of a load sufficient to achieve half of the strain at the onset of the cumulative fracture process or a minimum strain of 0.05 %, was met with the 30 MPa preloading.

The alignment procedure was checked with the isotropic aluminum sample of perfect geometry with a thickness of 4.10 mm and a gauge width of 3.6 mm. The sample was repeatedly loaded to about 53 MPa and the corresponding strains were determined at the up and down (Fig. 6, blue lines) as well as the left and the right (Fig. 6, red lines) measurement positions on the surface. The differences between the strains of the up-down and left-right measurement positions were used to determine deviations from nonhomogeneous axial strain states. The mean up/down strain difference was 0.11 µm with a maximum strain difference of 0.13 µm (Fig. 6**b**). It was further found that the maximum difference of axial strain between left and right measurement positions was only 0.21 µm (Fig. 6**c**), whereby the calculated mean strain difference of 0.07 µm corresponding to a PB value of only 0.6 %. The aluminum reference sample thus met both alignment criteria. The strains of left and right measurement positions as well as the strains of up and down positions did overlap. Hence, the measured strain difference of the aluminum dummy sample was in the range of the maximum measurement resolution of the used optical measurement device (laserXtens). The results of the aluminum dummy empirically confirmed

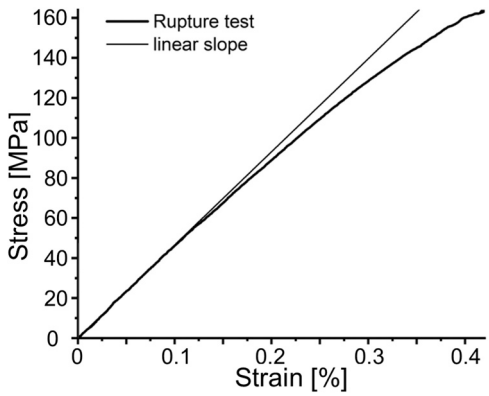

Fig. 4. Typical stress-strain curve of a C/C-SiC sample with monotonic loading up to failure. The linear slope highlights the deviation from a linear elastic material behavior above a stress of about 50 MPa.

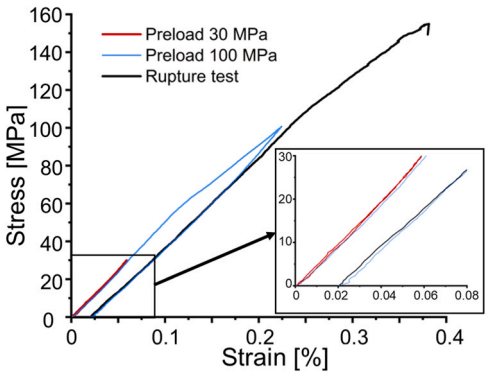

Fig. 5. Stress-strain curve of a C/C-SiC sample loaded to 30 MPa (red) and 100 MPa (blue) prior final tensile testing (black) with almost ideal elastic behavior after 30 MPa loading but clear signs of permanent strain after 100 MPa loading.

the high sensitivity and applicability of the alignment measurement described in Section 2.3. Furthermore, it also clearly showed the level of alignment achieved by the alignment tensile testing device when excluding deviations due to errors of as received surfaces or anisotropy of the tested material.

3.2. Microstructure and as received surface of C/C-SiC samples

Fig. 7a exhibits a characteristic microstructure of the C/C-SiC achieved from the LSI manufacturing [33–35] with a thermoplastic matrix precursor [29,36,37]. The bundle segments of the carbon fiber reinforced carbon (C_f/C) oriented in the 0° and 90° directions were surrounded by thin layers of grey SiC. The white silicon that did not react to form SiC can be found in the regions of former pores and cracks. The different phases, the anisotropy due to fiber bundle orientation, roughness, as well as small cracks and pores are typical for the inhomogeneity of the C/C-SiC surface. This inhomogeneity did not affect the speckle pattern observation for the optical strain measurement used in this study. By contrast, for the application of physical attached strain gauges it is recommended to apply treatments like surface filling and to use strain gauges with dimensions of not less than 6–12 mm to overcome the localized strain effects of the beforementioned inhomogeneities [27]. However, the use of such large strain gauges would not have allowed an alignment determination with samples of a gauge section of 2.52–4.95 mm width.

One objective of this study was to achieve tensile testing and alignment of samples in the as received surface condition. The roughness of the as received surfaces (Fig. 7**b**) resulted in line and point contacts between the centering brass inserts and the samples (Fig. 7c). This kind of contact limited the absolute positioning accuracy to about 50 µm. As a

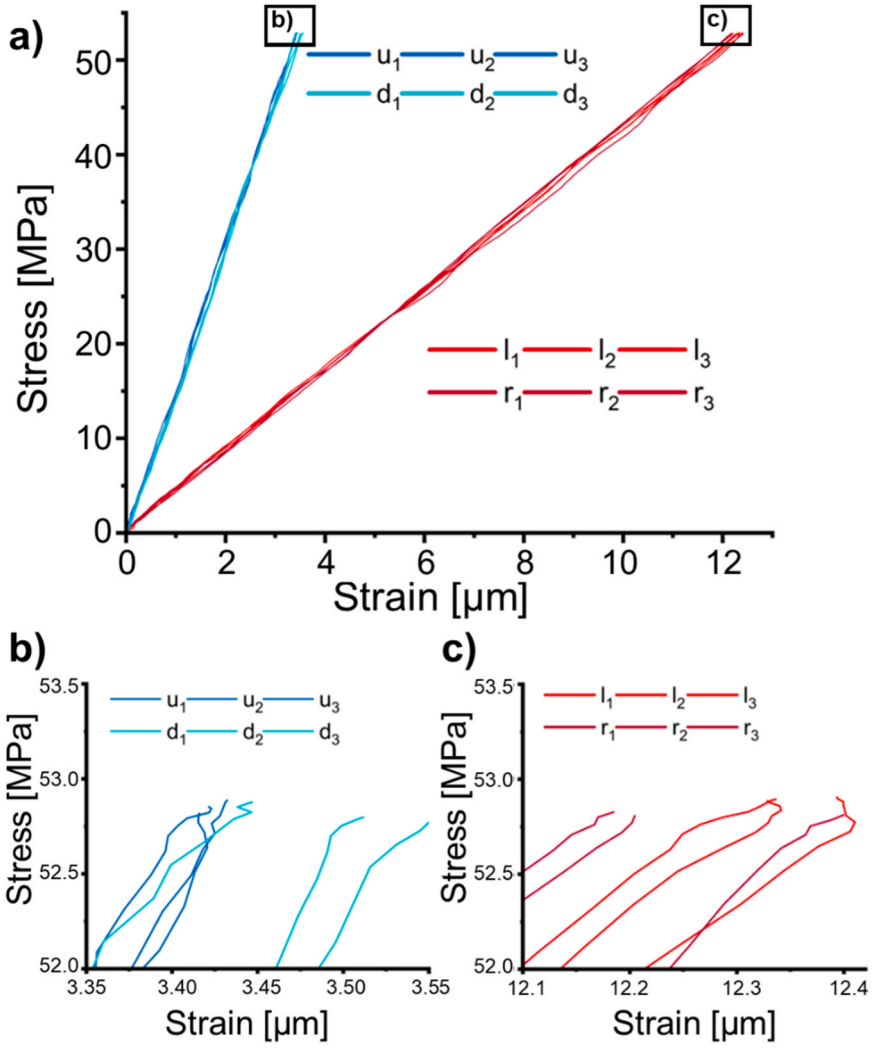

Fig. 6. The alignment check with the aluminum sample, which was preloaded in the elastic region several times to ~53 MPa, demonstrated a perfect alignment with very small strain deviations between b) the up (u_1-u_3) and down (d_1-d_3) and c) the left (l_1-l_3) and right (r_1-r_3) measurement positions.

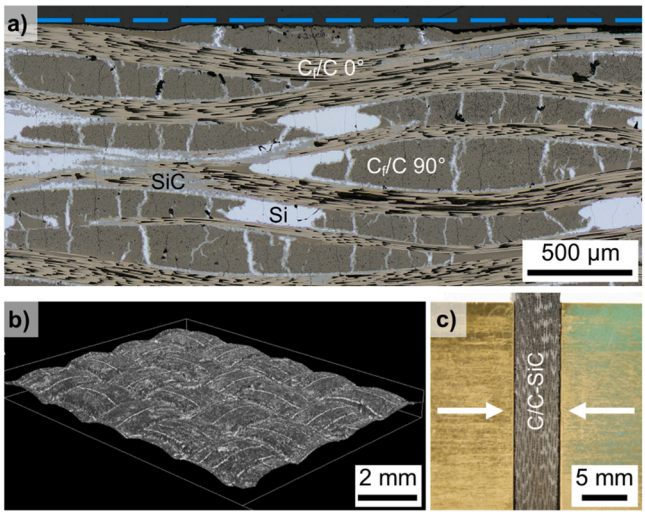

Fig. 7. a) Cross-section of the C/C-SiC sample with a characteristic phase composition and microstructure - the blue dashed line highlights the deviation of the sample surface from a smooth surface; b) 3-D light microscopy of as received C/C-SiC with weave structure on the surface; c) The yellow-golden brass inserts centered the tensile sample trough line and point contacts.

consequence, the re-mounting of the samples in the gripping allowed change of the absolute positioning until a minimum of misalignment was measured.

3.3. Influence of valid and invalid failure on the strength data of C/C-SiC

The verification of alignment prior failure testing of every single C/C-SiC tensile sample showed that far less than 15 % of the samples fulfilled both alignment criteria after their very first assembly in the testing device. More than 30 % of the samples finally achieved a compliance with alignment after several re-mountings of the samples in the testing device. Even so, it was not possible to be in accordance with both alignment criteria for all samples after the re-mounting and alignment procedure. However, all 92 samples were tested to evaluate the alignment criteria. Table 1 summarizes the results of the tensile tests. Samples found in compliance with alignment did achieve both alignment criteria. More than 96 % of these samples exhibited valid failure within the gauge section. Only one of these samples was invalid with a failure within the gripping. This kind of failure was only observed once for all of the tested samples and appeared to be a manufacturing defect of the sample. Samples not passing both alignment criteria were classified as misaligned. A misalignment was measured prior final testing for 97 % of the samples invalidly tested with a failure outside the gauge length. Hence, the rate of successful forecasting of valid and invalid testing with the alignment method was highly successful.

Fig. 8 shows the locations of the final failure of the tensile samples. No preferred failure was found between a location of fracture up or down from the center of the sample. The failure locations are displayed for both used sample geometries with the same gauge length of 20 mm as distance from the sample center. Thus, samples did fail valid within the gauge section up to a distance from the sample center below 10.0 mm (Fig. 8**a**). About 54 % of the valid samples failed within the first half of the gauge length. No preferred location of fracture was found for the validly tested samples. Invalidly tested samples failed outside the gauge section with a distance of fracture location of 10.0 mm and above (Fig. 8**b**). The transition radius of the samples ends at a distance of 16.00 mm and 17.34 mm for the smaller shaped and the bigger shaped samples, respectively. In total only one of the smaller shaped samples failed outside the transition radius at a distance of 16.55 mm within the gripping. Consequently, the absolute majority of the invalid samples failed within the transition radius. About 74 % of the failure locations of invalid samples occurred to a distance of 13.3 mm. Hence, the invalid samples fail outside of the end of the gauge section within the first half of the transition radius.

Table 1
Amount of the 92 total tested samples failing inside or outside the gauge section with regard to alignment.

	Compliance of alignment	Misalignment
Failed within gauge section	28	30
Failed outside gauge section	1*	33

* Outlier failed within the edge-loading shoulder gripping.

The evaluation of the influence of the tested sample size on the strength was not the objective of this study. This ongoing research will be discussed in a future publication. For the smaller shaped samples with 3.6 mm gauge width, enough samples were tested within this study to compare the strength data of validly tested samples with the strength of samples failing outside the gauge section (Table 2). The strength of the samples failing outside the gauge section was calculated from the maximum force at failure divided by the cross section at failure position within the transition radius of the sample.

It was found that the mean strength did not change for samples with a thickness of 2.52 mm (Fig. 9a). For samples with the larger thickness of 4.95 mm a very slightly decrease of strength from 163.6 to 156.5 MPa was measured (Fig. 9b). However, this strength decrease will pass a significance test only with a level of confidence less than 98 %. Hence, there was none or only a very slight tendency of strength decrease considering the data derived from failure outside the gauge section. By contrast, the standard deviations of strength between valid and invalid tests were different (Table 2). The standard deviation strongly increased for the invalid samples by 59.1 % and 53.7 % for samples with 2.52 mm and 4.95 mm thickness, respectively. Thus, the invalid samples showed an increase of scattering of more than 50 %.

As a result, the determination of the mean strength of C/C-SiC appeared to be very robust against misalignment. Consequently, strength measured by tensile testing qualifies as a suitable method for quality control and materials development. On the other hand, it was reported that brittle monolithic ceramics sometimes exhibited strength decrease with increased amount of percentage bending during tensile testing [22,23]. Nevertheless, it is not recommended to use the data of C/C-SiC samples failing outside the gauge section for modeling or methods of probabilistic failure prediction [41–43]. The high observed scattering would otherwise be a major source of uncertainty.

3.4. Influence of the alignment on valid tensile testing of CMC samples

The histogram in Fig. 10 summarizes the percentage bending determined before tensile testing and after the alignment procedure for all the samples failed valid. The distribution reveals that validly tested samples did not occur in the class with PB of more than 14 % and the majority of 80 % of validly tested samples were in the classes of PB values less than 6 %. The increase of PB gradually decreased the observed frequency of validly tested samples. Furthermore, the rate of valid testing, the PB value, and the measured up and down criterion were independent from the contour geometry or the thickness of the samples.

The tested samples were divided into three failure categories to correlate the influence of sample failure with the measured alignment criteria: a) The first category included the samples with valid failure and which fulfilled the alignment criteria before testing. b) The total of all samples with valid failure within the gauge section were in the second category. c) The last category merged samples with invalid failure, which did not achieve the alignment criterion before testing.

For the criterion of percentage bending the valid samples with compliance of alignment had a low mean PB of 2.7 % and an upper quartile of only 4.0 % (Fig. 11a). It has to be considered that all the 58

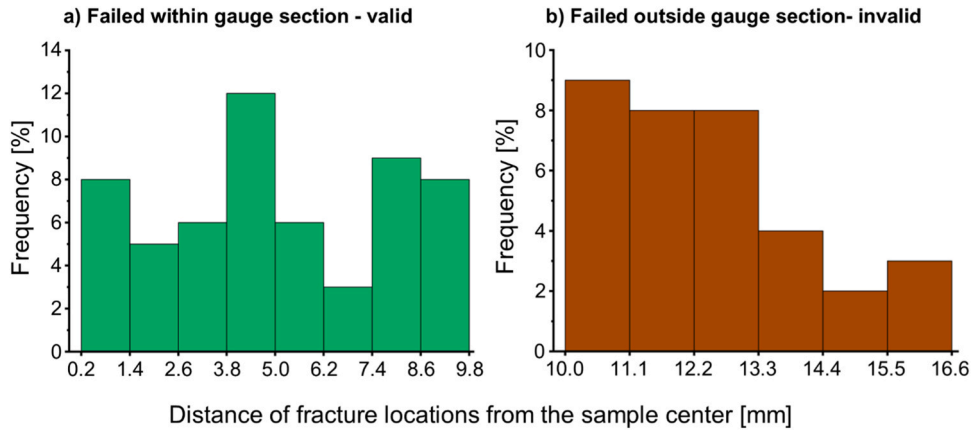

Fig. 8. Frequency of failure locations as distance from the sample center for samples failed a) valid and b) invalid.

Table 2
Strength data of samples with a gauge width of 3.6 mm failed valid or invalid.

	Mean strength [MPa]	Standard deviation [MPa]
Valid, 2.52 mm	159.1	4.4
Invalid, 2.52 mm	159.2	7.0
Valid, 4.95 mm	163.6	5.4
Invalid, 4.95 mm	156.5	8.3

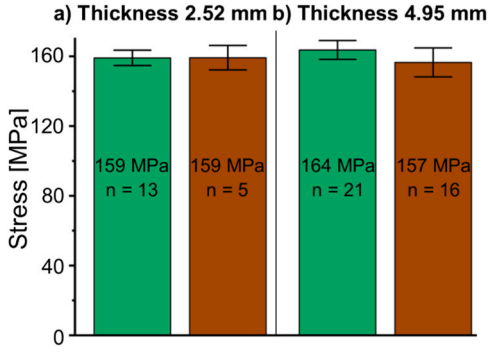

Fig. 9. Strength comparison of the samples failing within (green) or outside (brown) the gauge section for samples with a gauge width of 3.6 mm and a thickness of a) 2.52 mm and b) 4.95 mm.

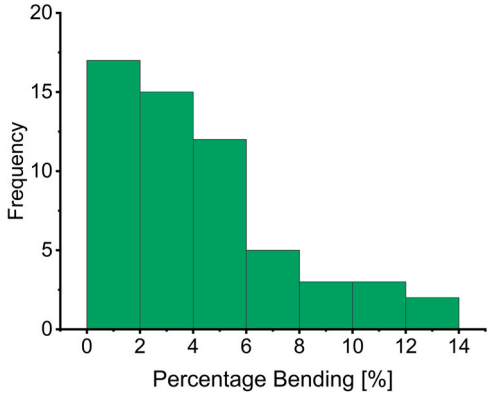

Fig. 10. Distribution of the measured percentage bending (PB) for all samples failing within the gauge section showed that about 80 % of valid samples had PB values of less than 6 %.

validly tested samples increased the mean PB to 4.2 % and the upper quartile to 5 % (Fig. 11b). The highest measured PB for a valid sample was 12.3 %. The invalid samples had a mean PB of 9 % with a lower quartile of 6.2 % (Fig. 11c). Although no sharp threshold for the transition from valid to invalid testing was found, the region between the upper quartile of 5.0 % for the valid samples and the lower quartile of 6.2 % for invalid samples can be addressed as a transition zone. Hence, a percentage bending above 6 % marked the point at which the invalid testing becomes predominant compared to valid testing, which was only slightly higher than the existing 5 % PB criterion currently recommended for ceramic matrix composites [27]. Moreover, the mean PB of invalid samples was more than two times higher compared to the mean value of valid samples and more than three times compared to the mean PB value for valid samples with compliance of alignment. Thus, the precheck and alignment procedure presented in this study led to clear measurement distinctions to predict both valid and invalid testing.

Fig. 12 depicts the measurement results for the up/down strain difference criterion. The valid samples that passed the alignment criterion had a mean strain difference of only 0.20 μm and an upper quartile of 0.30 μm (Fig. 12a), which was far below the set up/down threshold criterion of 0.45 μm. The up/down strain difference of all validly tested samples showed a mean of 0.47 μm (Fig. 12b). By contrast, the invalidly tested samples achieved a mean value about two times higher than the value of valid samples with a strain difference of 0.90 μm (Fig. 12c). Hence, the up and down criterion was able to determine a prediction of valid and invalid samples. Compared to the PB criterion, the measured difference between valid and invalid sample alignment was less pronounced for the up and down criterion. It was found that all validly tested samples with an upper quartile of 0.61 μm had a slightly overlap with the lower quartile at 0.54 μm of the invalid samples. The PB criterion showed a clearer selectivity than the up/down criterion due to the optical measurement system. The majority of misalignments measured for the PB and the up/down criteria came from the sample itself in terms of an offset in the gripping, cross sectional changes due to thickness changes, slightly curvature, and inner inhomogeneity. In contrast, only the up/down measurement can be influenced by biased strain reading of the optical measurement system, which is triggered if the sample moves in the direction to or apart from the camera in terms of tilting [31,44]. That could superimpose the strain measurement. Hence, it couldn't be distinguished between a movement of the sample and a difference in the strain. Nevertheless, in each case a determined difference of the up and down strains could be the cause of an invalid testing. Consequently, the difference of up and down strain rate was found to be a useful second criterion for the precheck of sample alignment. Although it was not as robust and informative as the percentage bending criterion, it was still responsible to determine 33 % of the invalid samples that did not met the alignment criterion before testing.

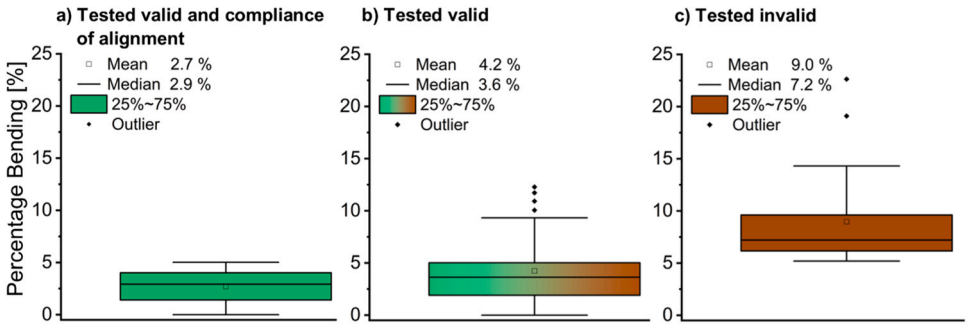

Fig. 11. Comparison of the percentage bending measurements of three sample categories: a) Samples failing within the gauge section with compliance of alignment, b) All samples failing in the gauge section, and c) Samples failing outside the gauge section.

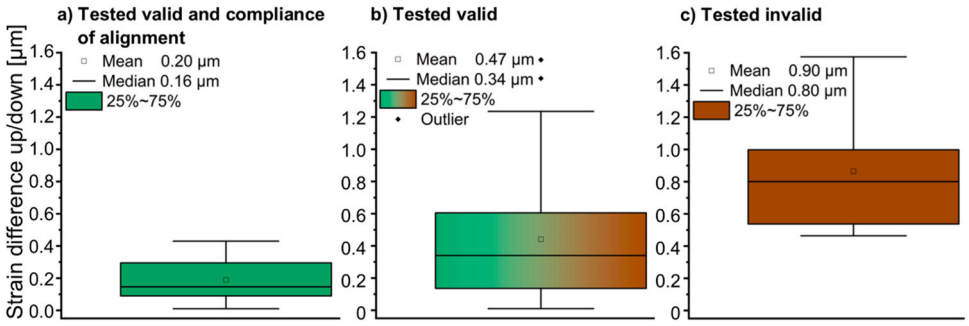

Fig. 12. Comparison of the up and down strain difference measurements of three sample categories: a) Samples failing in the gauge section with compliance of alignment, b) All samples failing in the gauge section, and c) Samples failing outside the gauge section.

More than 96 % of the tensile samples which passed both alignment criteria were tested with a valid failure in the gauge section. Conversely, 97 % of the invalid samples that failed outside the gauge length did at least failed for one of the two precheck criteria. Hence, the alignment checks prior testing achieved a highly reliable prediction. Finally, more than 60 % of all tested samples were tested validly after the alignment procedure and the remounting of the samples. This also included the samples that were tested despite not complying with the alignment criteria and were therefore expected to fail outside the gauge section. Only less than 15 % of the samples passed the alignment criteria without remounting. Consequently, it can be estimated that the rate of validly tested samples within this study were increased by up to four times. Our proposed procedure was therefore a significant improvement applying this simple and fast alignment method. Since the number of test samples for tensile evaluation is often very limited when developing new CMC materials and processes, the alignment method can be consequently highly recommended. It is expected that increasing the rate of successful tested samples increases the learning rate and the overall outcome of CMC developments that are often driven by empirical design of experiments.

The alignment method developed in this study for C/C-SiC tensile samples with imperfections due to as received surfaces, can be of valuable interest if deviations from perfect sample geometry must be accepted. As a case in point, CMCs for aviation and space applications need to be tested after an application of an environmental barrier coating [18,19], or a coating to seal porosity [28]. The necessary pretreatment of CMC samples prior coating like sand blasting as well as the coating by atmospheric plasma spraying itself will lead to inevitable changes of sample shapes from the initial geometries [18,19]. It should be further emphasized that the alignment method used an optical measurement system that can still be used at high temperatures, at which glued strain gauges can no longer be applied.

4. Conclusions

This study described a nondestructive method to precheck the alignment of CMC tensile samples before final testing. This alignment check was carried out with a state-of-the-art optical strain measurement system. Hence, additional strain gauge attachments on the sample surface were unnecessary and the alignment of samples can be also tested at high-temperatures.

In this study carbon fiber-reinforced silicon carbide (C/C-SiC) tensile samples were preloaded at room temperature in the linear elastic stress region and the sample alignment was determined by strain measurement from one side. For this purpose, a percentage of bending and a strain difference between an up and down measurement position on the samples were derived. Samples which did not pass a minimum alignment level were remounted in the tensile test device with self-aligning components. It was assumed that the rate of validly tested C/C-SiC samples was increased by four times with this procedure. Our method is therefore highly useful to increase the rate of valid testing of CMC samples if only a few samples are available, or the testing of as received surfaces or thermal or environmental coating do not allow a further sample machining.

It was found that the CMC material C/C-SiC was somewhat less sensitive to misalignment than monolithic ceramics and the minimum requirements necessary for their testing [22,26,27]. Nevertheless, valid failure was not observed with an amount of percentage of bending higher than 12.3 %. Furthermore, the rate of validly tested samples strongly decreased for a measured percentage bending above 6 %.

In addition, it was found that failure within or outside the gauge section resulted only in minimal deviations of the calculated nominal tensile strength for the C/C-SiC material. However, the scattering of the strength data increased by more than 50 % for failure outside the gauge section.

CRediT authorship contribution statement

Stefan Flauder: Writing – original draft, Investigation, Funding acquisition, Conceptualization. **Nico Langhof:** Writing – review & editing. **Stefan Schafföner:** Writing – review & editing, Resources.

Declaration of Competing Interest

The authors declare that they have no known competing financial interests or personal relationships that could have appeared to influence the work reported in this paper.

Acknowledgement

This work was supported by the German Research Foundation (DFG) [project grant number: 503759358].

Appendix A. Supporting information

Supplementary data associated with this article can be found in the online version at doi:10.1016/j.jeurceramsoc.2024.117001.

References

[1] K.K. Chawla, Ceramic Matrix Composites, in, in: K.K. Chawla (Ed.), Composite Materials Science and Engineering, Springer, Birmingham, 2019, pp. 251–295, https://doi.org/10.1007/978-3-030-28983-6_7.
[2] A.G. Evans, F.W. Zok, The physics and mechanics of fibre-reinforced brittle matrix composites, J. Mater. Sci. 29 (1994) 3857–3896, https://doi.org/10.1007/BF00355946.
[3] X. Wang, X. Gao, Z. Zhang, L. Cheng, H. Ma, W. Yang, Advances in modifications and high-temperature applications of silicon carbide ceramic matrix composites in aerospace: A focused review, J. Eur. Ceram. Soc. 41 (2021) 4671–4688, https://doi.org/10.1016/j.jeurceramsoc.2021.03.051.
[4] Q. Diao, H. Zou, X. Ren, C. Wang, Y. Wang, H. Li, T. Sui, B. Lin, S. Yan, A focused review on the tribological behavior of C/SiC composites: present status and future prospects, J. Eur. Ceram. Soc. 43 (2023) 3875–3904, https://doi.org/10.1016/j.jeurceramsoc.2023.03.002.
[5] J. Steibel, Ceramic matrix composites taking flight at GE aviation, Am. Ceram. Soc. Bull. 98 (2019) 30–33.
[6] K. Ranasinghe, K. Guan, A. Gardi, R. Sabatini, Review of advanced low-emission technologies for sustainable aviation, Energy 188 (2019) 115945, https://doi.org/10.1016/j.energy.2019.115945.
[7] P. Wehrel, R. Schöffler, C. Grunwitz, F. Carvalho, M. Plohr, J. Häßy, A. Petersen, Performance and emissions benefits of cooled ceramic matrix composite vanes for high-pressure turbines, J. Eng. Gas. Turbines Power 145 (2023) 121016, https://doi.org/10.1115/1.4063534.
[8] ASTM, Standard Test Method for Flexural Properties of Continuous Fiber-Reinforced Advanced Ceramic Composites. ASTM C1341-13. 2023. https://dx.doi.org/10.1520/C1341-13R23.
[9] ISO 17138:2014-12: Fine ceramics (advanced ceramics, advanced technical ceramics) - Mechanical properties of ceramic composites at room temperature - Determination of flexural strength. ⟨https://www.beuth.de/en/standard/iso-17138/227442708⟩.
[10] D. Sciti, S. Corradetti, M. Manzolaro, M. Ballan, D. Cesarotto, G. Meneghetti, L. Silvestroni, F. Servadei, L. Zoli, Highly porous carbon-SiC composites with continuous carbon fibers for the production of radioisotopes in ISOL facilities, J. Eur. Ceram. Soc. 44 (2024) 6854–6863, https://doi.org/10.1016/j.jeurceramsoc.2024.04.072.
[11] D. Sciti, L. Zoli, A. Vinci, L. Silvestroni, S. Mungiguerra, P. Galizia, Effect of PAN-based and pitch-based carbon fibres on microstructure and properties of continuous C_f/ZrB2-SiC UHTCMCs, J. Eur. Ceram. Soc. 41 (2021) 3045–3050, https://doi.org/10.1016/j.jeurceramsoc.2020.05.032.
[12] W. Freudenberg, F. Wich, N. Langhof, S. Schafföner, Additive manufacturing of carbon fiber reinforced ceramic matrix composites based on fused filament fabrication, J. Eur. Ceram. Soc. 42 (2022) 1822–1828, https://doi.org/10.1016/j.jeurceramsoc.2021.12.005.
[13] B. Baker, V. Rubio, P. Ramanujam, J. Binner, A. Hussain, T. Ackerman, P. Brown, I. Dautremont, Development of a slurry injection technique for continuous fibre ultra-high temperature ceramic matrix composites, J. Eur. Ceram. Soc. 39 (2019) 3927–3937, https://doi.org/10.1016/j.jeurceramsoc.2019.05.070.
[14] C. Zhang, P. Hu, L. Xun, J. Han, X. Zhang, A universal strategy towards the fabrication of ultra-high temperature ceramic matrix composites with outstanding mechanical properties and ablation resistance, Compos., Part B 280 (2024) 111485, https://doi.org/10.1016/j.compositesb.2024.111485.
[15] Y. Shi, Y. Xiu, P. Wu, C. Wang, Y. Xiao, R. Jemmali, D. Cepli, K. Tushtev, Notch sensitivity of C/C-SiC composite evaluated by flexural tests, J. Eur. Ceram. Soc. 44 (2024) 3139–3146, https://doi.org/10.1016/j.jeurceramsoc.2023.12.075.
[16] Y. Zhou, From properties of zirconium carbide to the reverse design of ultra-high temperature CMCs, J. Am. Ceram. Soc. 107 (2024) 7023–7037, https://doi.org/10.1111/jace.20016.
[17] M. Park, J. Gu, H. Lee, S.-H. Lee, L. Feng, W.G. Fahrenholtz, C_f/SiC Ceramic matrix composites with extraordinary thermomechanical properties up to 2000 °C, Nanomaterials 14 (2024) 72, https://doi.org/10.3390/nano14010072.
[18] M.B. Ruggles-Wrenn, T.M. Williams, Fatigue of a SiC/SiC ceramic composite with an ytterbium-disilicate environmental barrier coating at elevated temperature, Int. J. Appl. Ceram. Technol. 17 (2020) 2074–2082, https://doi.org/10.1111/ijac.13539.
[19] Z. Yang, W. Li, Y. Chen, W. Zeng, W. Chen, X. Cao, Life assessment of thermomechanical fatigue in a woven SiC/SiC ceramic matrix composite with an environmental barrier coating at elevated temperature, Int. J. Fatigue 172 (2023) 107584, https://doi.org/10.1016/j.ijfatigue.2023.107584.
[20] M. Mizuno, S. Zhu, Y. Nagano, Y. Sakaida, Y. Kagawa, M. Watanabe, Cyclic-fatigue behavior of SiC/SiC composites at room and high temperatures, J. Am. Ceram. Soc. 79 (1996) 3065–3077, https://doi.org/10.1111/j.1151-2916.1996.tb08078.x.
[21] B. Zeng, Q. Ma, Y. Xue, C. Liao, H. Qin, X. Chen, J. Hu, X. Zhang, J. Yang, S. Dong, Fatigue resistance and damage mechanisms of 2D woven SiC/SiC composites at high temperatures, Int. J. Appl. Ceram. Technol. 20 (2023) 3052–3063, https://doi.org/10.1111/ijac.14379.
[22] M.G. Jenkins, M.K. Ferber, R.L. Martin, V.T. Jenkins, V.J. Tennery, Study and Analysis of the Stress State in a Ceramic, Button-Head, Tensile Specimen, U.S. National Technical Information Service (1991) ORNL/TM-11767. https://doi.org/10.2172/814571.
[23] V.J. Tennery, K. Breder, M.K. Ferber, M.G. Jenkins, Tensile fracture behavior of two types of silicon nitride specimen geometries conducted by Ten U.S. groups, J. Eur. Ceram. Soc. 83 (2000) 1186–1191, https://doi.org/10.1111/j.1151-2916.2000.tb01352.x.
[24] J. Bessers, A code of practice for the measurement of misalignment induced bending in uniaxially loaded tension-compression test pieces. European Commission, Directorate-General for Research and Innovation, Joint Research Centre 1995, ISBN 92-826-9681-2. ⟨https://op.europa.eu/en/publication-detail/-/publication/9c0d0257-8b30-11e9-9369-01aa75ed71a1⟩.
[25] B.W. Christ, S.R. Swanson, Alignment problems in the tensile test, J. Test. Eval. 4 (1976) 405–417, https://doi.org/10.1520/jte11371j.
[26] ISO 17161:2016-10: Fine ceramics (advanced ceramics, advanced technical ceramics) - Ceramic composites - Determination of the degree of misalignment in uniaxial mechanical tests. https://www.dinmedia.de/de/norm/din-en-iso-17161/253116243.
[27] ASTM, Standard Test Method for Monotonic Tensile Behavior of Continuous Fiber-Reinforced Advanced Ceramics with Solid Rectangular Cross-Section Test Specimens at Ambient Temperature, ASTM C1275-18. 2018:1–21. https://doi.org/10.1520/C1275-18.
[28] R. Krishna, V.K. Parimi, A. Udayakumar, R. Mitra, Evaluation of elastic constants and high temperature tensile behaviour with damage assessment of the SiC seal-coated 2.5D Cf/SiC composites having multilayered interphase and Si-B-C added matrix, J. Eur. Ceram. Soc. 43 (2023) 2388–2401, https://doi.org/10.1016/j.jeurceramsoc.2022.12.066.
[29] S. Flauder, I. Bombarda, R. D'Ambrosio, N. Langhof, A. Lazzeri, W. Krenkel, S. Schafföner, Size effect of C/C-SiC: Part 2 - tensile testing with alignment device, J. Eur. Ceram. Soc. 42 (2022) 1227–1237, https://doi.org/10.1016/j.jeurceramsoc.2021.11.044.
[30] D. Amodio, G.B. Broggiato, F. Campana, G.M. Newaz, Digital speckle correlation for strain measurement by image analysis, Exp. Mech. 43 (2023) 396–402, https://doi.org/10.1007/BF02411344.
[31] E. Schenuit, R. Bolkart, T. Becker, O. Spinka, Optical strain measurement on small specimens based on laser speckles, Mater. Sci. Forum 584-586 (2008) 237–242, https://doi.org/10.4028/www.scientific.net/msf.584-586.237.
[32] P. Reynaud, C. Tallaron, A. Cosculluela, C. Cambas, P. Gomez, J.L. Delamaide, M. Bourgeon, Measurement of bending in specimens of Ceramic-matrix composites uniaxially loaded in tension-compression, Proceedings of the International Conference on Composite Materials-ICCM-12. (1999) paper1345. ⟨https://www.iccm-central.org/Proceedings/ICCM12proceedings/papers/pap1345.pdf⟩.
[33] D. Kopeliovich, Advances in the manufacture of ceramic matrix composites using infiltration techniques, in: I.M. Low (Ed.). Advances in Ceramic Matrix Composites, Woodhead Publishing, Oxford, 2014, pp. 79–108, https://doi.org/10.1533/9780857098825.1.79.
[34] P.J. Hofbauer, F. Raether, E. Rädlein, Finite element modeling of reactive liquid silicon infiltration, J. Eur. Ceram. Soc. 40 (2020) 251–258, https://doi.org/10.1016/j.jeurceramsoc.2019.09.041.
[35] M. Naikade, A. Ortona, T. Graule, L. Weber, Liquid metal infiltration of silicon based alloys into porous carbonaceous materials. Part I: modelling of channel filling and reaction phase formation, J. Eur. Ceram. Soc. 42 (2022) 1971–1983, https://doi.org/10.1016/j.jeurceramsoc.2021.12.068.
[36] F. Reichert, N. Langhof, W. Krenkel, Influence of thermal fiber pretreatment on microstructure and mechanical properties of C/C-SiC with thermoplastic polymer-derived matrices, Adv. Eng. Mater. 17 (2015) 1119–1126, https://doi.org/10.1002/adem.201500193.
[37] S. Flauder, N. Langhof, W. Krenkel, S. Schafföner, Size effect of C/C-SiC: Part 1 - bending load and statistical effects, J. Eur. Ceram. Soc. 41 (2021) 6805–6814, https://doi.org/10.1016/j.jeurceramsoc.2021.07.040.
[38] M. Moos, C. Möhl, R. Reichert, G. Ohnemüller, N. Langhof, S. Baz, T. Opel, G. T. Gresser, S. Schafföner, Novel approach for ceramic matrix composites – Cf/PEEK hybrid yarn-based C/C-SiC, J. Eur. Ceram. Soc. 44 (2024) 130–141, https://doi.org/10.1016/j.jeurceramsoc.2023.09.005.

[39] C. Wei, L. Zhao, D. Hu, J. Ni, Electrical discharge machining of ceramic matrix composites with ceramic fiber reinforcements, Int. J. Adv. Manuf. Technol. 64 (2013) 187–194, https://doi.org/10.1007/s00170-012-3995-5.
[40] ZwickRoell, LaserXtens 2-120 HT TZ, https://www.zwickroell.com/accessories/extensometers/laserxtens/laserxtens-2-120-hptz/#c67490, 2024 (accessed 01 Aug 2024).
[41] R. Danzer, T. Lube, P. Supancic, R. Damani, Fracture of ceramics, Adv. Eng. Mater. 10 (2008) 275–298, https://doi.org/10.1002/adem.200700347.
[42] R.A. Heller, S. Thangjitham, I. Yeo, Reliability and failure analyses of 2-D Carbon-Carbon structural components, Air Force OLAC Tech. Rep. (1992). PL-TR-91-3068.
[43] J.C. McNulty, F.W. Zok, Application of weakest-link fracture statistics to fiber-reinforced ceramic-matrix composites, J. Am. Ceram. Soc. 80 (1997) 1535–1543, https://doi.org/10.1111/j.1151-2916.1997.tb03013.x.
[44] M. Štěpánek, M. Zahálka, J. Mach, V. Mentl, Z. Bunda, J. Volák, The Measurement of longitudinal deformation of miniature test specimens, 26th International Conference on Metallurgy and Materials, (2018) p.1015-19. ⟨https://www.proceedings.com/47138.html⟩.